Original Article

Early diagnostic and prognostic value of myocardial strain derived from cardiovascular magnetic resonance in patients with cardiac amyloidosis

Weijie Hou[1#], Zhi Wang[1#], Jingzhou Huang[1], Fangfang Fan[1], Fan Yang[1], Lin Qiu[1], Kai Zhao[2], Jianxing Qiu[2], Ying Yang[1,3], Wei Ma[1], Yanjun Gong[1], Tao Hong[1]

[1]Department of Cardiology, Peking University First Hospital, Beijing, China; [2]Department of Radiology, Peking University First Hospital, Beijing, China; [3]Echocardiography Core Laboratory, Institute of Cardiovascular Disease, Peking University First Hospital, Beijing, China

Contributions: (I) Conception and design: Y Gong, Z Wang, T Hong; (II) Administrative support: F Yang, L Qiu; (III) Provision of study materials or patients: None; (IV) Collection and assembly of data: J Huang; (V) Data analysis and interpretation: Y Yang, W Ma, K Zhao, J Qiu, J Huang, F Fan; (VI) Manuscript writing: All authors; (VII) Final approval of manuscript: All authors.

[#]These authors contributed equally to this work as co-first authors.

Correspondence to: Yanjun Gong, MD. Department of Cardiology, Peking University First Hospital, 8 Xishiku St., Xicheng District, Beijing 10034, China. Email: gongyanjun111@163.com.

Background: Cardiac amyloidosis (CA) is one of the causes of heart failure with preserved ejection fraction. Cardiac magnetic resonance (CMR) with late gadolinium enhancement (LGE) and extracellular volume (ECV) fractions is a preferred method to identify CA. However, the requirement of contrast limits its use in renal deficiency patients. Myocardial strain is a promising method without contrast. We sought to assess the early diagnostic and prognostic value of strain.

Methods: This retrospective study enrolled 31 patients with systemic amyloidosis (SA) in Peking University First Hospital from January 2014 to January 2019. The patients were categorized into three groups, including 11 CA patients with left ventricular hypertrophy (CA-LVH group), 9 CA patients without LVH (CA-NLVH group), and 11 patients with extracardiac SA (SA group). Strain analysis was performed with CMR images. A least absolute shrinkage and selection operator (LASSO) was used to generate strain score. The receiver operating characteristic (ROC) curve was used to evaluate the early diagnostic efficacy of strain score and other single strain parameter. The primary endpoint was defined as death from all cause or rehospitalization for heart failure. A Cox proportional hazards model was used to assess the index value on the prognosis.

Results: In CA patients, as the left ventricular wall thickens, the global and regional strain decrease significantly. A new strain score (strain score = 0.00893 × mid-septal circumferential peak strain + 0.02285 × apical radial peak strain + 0.1541 × apical circumferential peak strain + 0.33097 × epicardial circumferential average peak strain + 0.42232 × endocardial longitudinal average peak strain) generated using LASSO showed that the area under the ROC curve was 0.909. All the patients with outcome events were in CA groups, four were in CA-LVH group and one in CA-NLVH group. New York Heart Association (NYHA) grade [hazard ratio (HR) =14.29, 95% confidence interval (CI): 2.34–87.34, P<0.01], brain natriuretic peptide (HR =20.05, 95% CI: 2.21–182.36, P=0.008), cardiac injury biomarker (HR =11.59, 95% CI: 1.03–130.36, P=0.047), E/E' (mitral inflow to mitral relaxation velocity ratio) (HR =1.09, 95% CI: 1.00–1.18, P=0.040), end-systolic left ventricular volume (HR =1.04, 95% CI: 1.00–1.18, P=0.039) and LGE volume (HR =1.11, 95% CI: 1.02–1.20, P=0.012) positively correlate with events. Better renal function (HR =0.92, 95% CI: 0.86–0.98, P=0.011) and ejection fraction (HR =0.94, 95% CI: 0.88–0.99, P=0.027) appear to be protective factors. Although with no statistical difference, the strain damage had a tendency to predict poor prognosis, i.e., mid-ventricular circumferential strain with HR of 1.25 (95% CI: 1.0–1.57, P=0.050) and strain score with HR of 1.30 (95% CI: 0.98–1.73, P=0.067).

Conclusions: Myocardial strain decreased in CA patients. The integrated magnetic resonance imaging (MRI) strain score can serve as a useful tool to identify early myocardial involvement in amyloidosis. The strain damage had a tendency to predict poor prognosis.

Keywords: Cardiac amyloidosis (CA); heart failure; myocardial strain; echocardiography; cardiac magnetic resonance (CMR)

Submitted May 10, 2023. Accepted for publication Oct 13, 2023. Published online Nov 23, 2023.
doi: 10.21037/cdt-23-205
View this article at: https://dx.doi.org/10.21037/cdt-23-205

Introduction

Systemic amyloidosis (SA) is an infiltrating disease with pathogenesis as continuous infiltration of various amyloid substances in multiple organs of the human body. This infiltration can cause organ dysfunction and even lead to death in severe cases. SA is a rare disease with an incidence of 8–14 cases per million people (1,2). SA can be divided into many subtypes based on the different compositions of amyloid. More than 30 types of amyloid precursor proteins have been identified (3). Based on the different organs involved, it can be divided into skin amyloidosis, renal amyloidosis, peripheral nerve amyloidosis, cardiac amyloidosis (CA) and other different types. Different organs may be affected at the same time (4).

When amyloid material affects the heart, it is called CA. Heart involvement in amyloidosis often indicates a poor prognosis. Progressive amyloid deposition can lead to restrictive cardiomyopathy, episodes of arrhythmia and severe conduction disturbances, including atrioventricular block with syncope or sudden death (5). There are two types of amyloidosis that are most likely to affect the heart, namely light chain amyloidosis (AL) and transthyretin (TTR) amyloidosis (6). In the past, the lack of understanding of this disease by clinicians led to many misdiagnoses and missed diagnoses of patients, and the lack of interventions led to a very poor prognosis. In recent years, the diagnosis and treatment of the two subtypes of CA have been continuously improved. Early detection and diagnosis of CA and appropriate treatment are of great significance for improving the prognosis of the patients.

At present, in addition to the classical methods for the diagnosis of CA, including clinical manifestations, electrocardiogram (ECG), and echocardiography, the most important non-invasive assessment is cardiac enhanced magnetic resonance, and late gadolinium enhancement (LGE) sequence, extracellular volume (ECV) fractions, T1 mapping and T2 mapping of this examination (7-11). The presence or absence of LGE and the range of delayed enhancement can help doctors to detect CA and assess its severity (12-14). The increase in ECV can help early detection of CA, assist in diagnosis, and provide prognostic information (15). However, in patients with severe heart failure or renal insufficiency, the contraindication of gadolinium contrast agent may limit the use of LGE and ECV. T1 mapping has high application value in the diagnosis and differentiation of CA and does not require the use of contrast agents, and it can also be applied in patients with renal deficiency. However, it is difficult to perform carry out in most hospitals. Therefore, it is critical to explore imaging methods that can detect cardiac involvement earlier without the use of contrast agents. Strain is the sum of local cardiac motion. It has been suggested that a reduction in myocardial strain can occur early in the course of CA prior to LGE-positive (5). Early changes in strain can be very sensitive when the heart is

Highlight box

Key findings

- There is evidence of impaired myocardial stress in patients with cardiac amyloidosis (CA), which is an indicator of poorer prognosis. A new strain score may indicate early myocardial involvement in patients with amyloidosis.

What is known and what is new?

- Myocardial strain decreased in CA patients. And strain damage had a tendency to predict poor prognosis.
- Strain score may improve the efficiency of early diagnosis and differential diagnosis in patients with systemic amyloidosis.

What is the implication, and what should change now?

- Further large clinical trials need to address the tendency of strain injury to predict poor prognosis.

involved and can be obtained without the application of contrast agent, making it a promising method to detect early involvement of the heart in amyloidosis (5,16,17).

Strain refers to the percentage of deformation of the myocardial fiber relative to its original length. Based on different directions of myocardial deformation, it can be divided into radial strain, circumferential strain and longitudinal strain. Myocardial strain can sensitively reflect the myocardial motor function and quantitatively analyze the overall and local myocardial motion. Recently, strain has been rapidly developed in the field of CMR, and importantly, it does not require the application of contrast agents (18,19). Previous studies focused on various strains without integration to optimize their values. To date, few studies have focused on the early detection of CA cardiac involvement using strain while the wall thickness is still normal (5,20). The purpose of this study is to evaluate strain changes in patients with CA and to try to establish a model that can assist in early detection of CA cardiac involvement without contrast agents when wall thickness is still normal. We present this article in accordance with the STROBE reporting checklist (available at https://cdt.amegroups.com/article/view/10.21037/cdt-23-205/rc).

Methods

Population

This study retrospectively enrolled 53 patients diagnosed with SA in Peking University First Hospital from January 2014 to January 2019. Cardiac enhanced magnetic resonance was performed in 33 patients. One patient with severe renal insufficiency and another with left bundle branch block were excluded. Thus, a total of 31 patients with SA were included in the analysis, including 20 patients with LGE (including 11 patients with left ventricular hypertrophy, 9 patients without left ventricular hypertrophy) and 11 patients without LGE. The study was conducted in accordance with the Declaration of Helsinki (as revised in 2013). The study was approved by the Ethics Committee of Peking University First Hospital (No. 2020keyan141). Written consent was waived owing to the minimal patient risk in accordance with the relevant guidelines and regulations of Peking University First Hospital Ethics Committee, but all patients were consented for the procedure.

Inclusion criteria

Amyloidosis: the diagnosis of amyloidosis was based on biopsy of tissues outside the heart (abdominal fat pad, rectum, kidney, bone marrow, tongue, labial glands, skin, etc.) that confirmed amyloid deposition (congo red staining under polarized light microscopy, showing apple green birefringence characteristics).

Findings of diffuse subendocardial or transmural LGE or focal and patchy LGE on CMR indicated CA, otherwise defined as SA without cardiac involvement. The CA group was then divided into a left ventricular hypertrophy group (CA-LVH) and a non-left ventricular hypertrophy group (CA-NLVH) according to whether the mean value of the thickness of the ventricular septum and free wall measured by echocardiography was greater than 12 mm.

Exclusion criteria

Exclusion criteria consist of presence of valvular disease, congenital heart disease, cardiomyopathy, severe coronary stenosis, history of myocardial infarction, acute heart failure, II–III atrioventricular block, left bundle branch block, severe renal insufficiency [estimated glomerular filtration rate (eGFR) <30 mL/min/1.73 m^2].

CMR imaging protocol

GE Discovery MR 750 3.0T (Signa Excite^{TM}; GE Medical System, Milwaukee, Wisconsis, USA) or Siemens AURA 1.5T (MAGNETOM Skyra, Siemens Healthineers, Erlangen, Germany) magnetic resonance imaging (MRI) system in Peking University First Hospital was used for imaging. Taking the GE MRI as an example, the 8-channel phased array coil is used for ECG-gated breath-hold scanning, and Realtime Loc is used for real-time heart positioning scanning to obtain left ventricular long-axis two-chamber, four-chamber and three-chamber heart (left ventricular outflow). Gated fast equilibrium steady-state precession gradient echo [fast imaging employing steady-state acquisition (FIESTA) cine] is used to obtain left ventricular long-axis two-chamber heart, four-chamber heart, left ventricular outflow tract level and 9–15 short-axis left ventricular film images. The scanning parameters are as follows: repetition time (TR) =3.6 ms, echo time (TE) =1.6 ms, flip angle =45°, imaging field of view (FOV) =380 mm × 380 mm, matrix =512×512, layer thickness =8 mm, layer spacing =0.

After acquisition of the movie sequence, the Ga-DTPA contrast agent is injected at a dose of 0.1 mmol/kg and a flow rate of 1 mL/s. After completion, 20 mL of 0.9% sodium chloride injection is added and a delayed enhancement sequence [myocardial delayed enhancement (MDE)] is performed after 15 minutes.

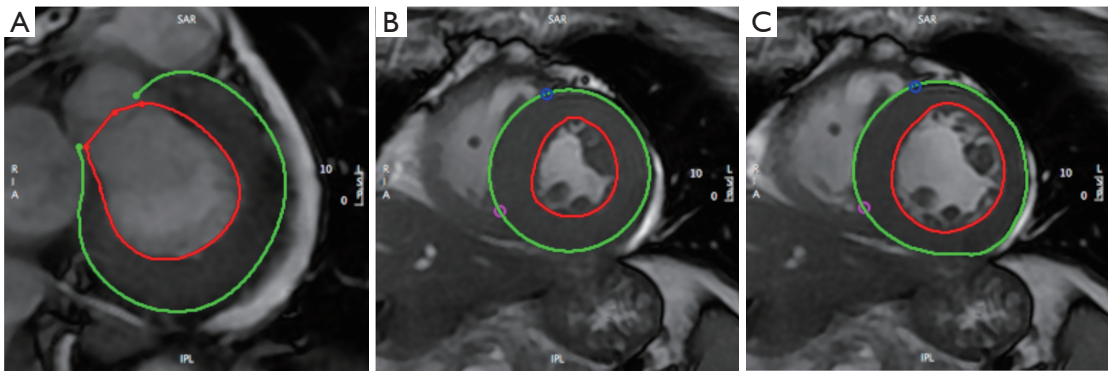

Figure 1 Short-axis level description of left ventricular endocardial and epicardial membrane. The red line and the green line define endocardial and epicardial borders.

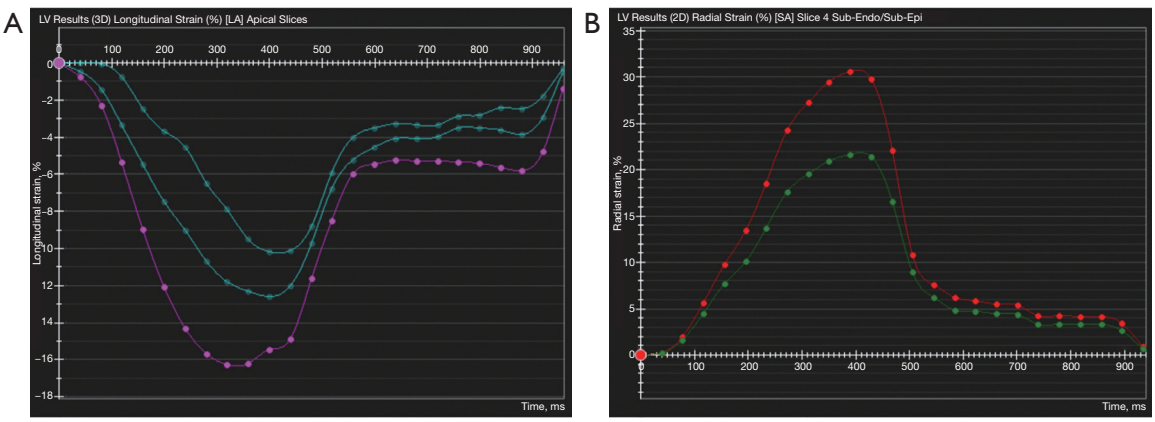

Figure 2 The color-coded strain graph shows the longitudinal strain result (A; the lines correspond to basal longitudinal peak strain, mid-septal longitudinal peak strain and apical longitudinal peak strain from top to bottom) and the radial strain result (B; the red line corresponds to endocardial radial average peak strain and the green line corresponds to epicardial radial average peak strain) of each segment *vs.* time. LV, left ventricular; 3D, three-dimensional; LA, long axis; 2D, two-dimensional; SA, short axis; Endo, endocardial; Epi, epicardial.

Strain analysis

Two senior doctors (J.Q. and K.Z. with more than 10 years of experience in CMR interpretation) were trained to use CMR post-processing software (Circle Cardiovascular Imaging 5.11.4, CVI42) for image post-processing. The CMR image is imported into the CVI42 software to automatically delineate the myocardial boundary (*Figure 1*).

The CVI42 software automatically tracks the trajectory of the inner and outer membranes during the cardiac cycle, automatically calculates the strain parameters with feature tracking (FT), and reads the following parameters from the report generated by the software:

(I) Global strain value: three-dimensional (3D) global longitudinal peak strain (GLS), circumferential peak strain (GCS) and radial peak strain (GRS);

(II) Strain result of each segment: 3D basal longitudinal peak strain (Basal-LS), circumferential peak strain (Basal-CS) and radial peak strain (Basal-RS); 3D mid-septal longitudinal peak strain (Mid-LS), circumferential peak strain (Mid-CS), radial peak strain (Mid-RS); 3D apical longitudinal peak strain (Apical-LS), circumferential peak strain (Apical-CS), radial peak strain (Apical-RS);

(III) Endocardial and epicardial strain result (*Figure 2*): including two-dimensional (2D) short-axis endocardial and epicardial circumferential average peak strain (Endo-CS, Epi-CS), 2D short-axis endocardial and epicardial radial average peak strain (Endo-RS, Epi-RS), 2D long-axis endocardial and

epicardial longitudinal average peak strain (Endo-LS, Epi-LS);

(IV) Calculate the relative regional strain ratio (RRSR), endo-epicardial strain difference (Endo–Epi), and endo-epicardial strain ratio (Endo/Epi) according to the following formula:
   (i) RRSR = 3D peak strain of the apical segment/3D peak strain of the basal segment + 3D peak strain of the middle septal;
   (ii) Endo–Epi = average peak strain of the short-axis endocardium – average peak strain of the short-axis epicardium;
   (iii) Endo/Epi = average peak strain of short-axis endocardium/average peak strain of short-axis epicardium.

Data collection

This study followed all enrolled amyloidosis patients. Patients' medical and family history, smoking and medications status, weight, height, and demographics were collected within the first 4 h of admission. And the primary endpoint of this study was defined as death from all cause or rehospitalization for heart failure. The follow-up information was obtained by a researcher searching medical records or making phone calls to patient or family members to ask if the patient had completed chemotherapy and/or hematopoietic stem cell transplantation. Follow-up ended in January 2020. Event-free survival time is defined as the number of months between the date of completion of cardiac magnetic resonance (CMR) imaging and the date of the primary endpoint event or the end of the follow-up.

Statistic analysis

SPSS 26.0, MedCalc 19.2, Empowerstates and R3.4.3 were used for data processing and statistical analysis. The measurement data are normally distributed by using the Shapiro-Wilk test. Normally distributed measurements are presented as mean ± standard deviation. Comparisons between two groups were performed using a two-tailed Student's *t*-test; for multiple groups a one-way anlysis of variance (ANOVA) with *post-hoc* Bonferroni analysis was used. Non-normally distributed parameters are presented as quartiles, and the Mann-Whitney *U* test or Kruskall-Wallis *H* test with *post-hoc* Bonferroni analysis was used for pairwise comparisons. Count data are expressed as numbers of cases and percentages. The fisher exact test was used for unordered categorical variables.

We used the R glmnet module of Empowerstates to perform the least absolute shrinkage and selection operator (LASSO) regression analysis to generate a formula: use the Lasso regression model for variable selection, use the cross-validation method to select λ. The formula was then used to calculate a score (named as strain score) for each patient. The receiver operating characteristic (ROC) curve was used to evaluate the early diagnostic efficacy of the strain score and other single strain parameters. Univariate Cox proportional hazards model was used to analyze the prognosis of patients with amyloidosis. For all indicators, $P<0.05$ indicates that the difference is statistically significant.

Results

Baseline

Of all 31 patients, 30 patients were diagnosed with light-chain amyloidosis and one patient in CA-NLVH group was diagnosed with amyloid A (AA) amyloidosis. The baseline characteristics of CA and non-cardiac SA are shown in *Table 1*. Compared with CA-NLVH patients, cardiac function was worse, brain natriuretic peptide (BNP) and cardiac injury biomarker [cardiac troponin (cTNI)] level was higher in CA-LVH patients. More limb lead low voltage in ECG was found in CA-NLVH patients than SA patients. There was no significant difference in other baseline characteristics.

Echocardiography

Routine echocardiography parameters were shown in *Table 2*. Greater left atrium anterior-posterior diameter (LA-APD) and left ventricular mass index (LVMI) was found in CA-LVH compared with CA-NLVH group. Meanwhile, the interventricular septum thickness (IVST) and left ventricular posterior wall thickness (LVPWT) were thicker in CA-LVH patients compared with CA-NLVH patients. Cardiac function was worse in both systolic and diastolic phase for CA-LVH patients. No difference in echocardiography parameters was found between CA-NLVH group and SA group.

CMR routine parameters

Routine CMR parameters were shown in *Table 3*. Thicker IVST, LVPWT and larger end-systolic volume (ESV) were found in CA-LVH group compared with CA-NLVH group. LVPWT was thicker in CA-NLVH group compared with SA group.

Table 1 Baseline characteristics of the three groups

Characteristic	CA-LVH (n=11)	CA-NLVH (n=9)	SA (n=11)	P value
Male (%)	72.7†	55.6§	36.4	0.230
Age (years)	55.8±8.5	51.8±8.1	55.7±7.1	0.432
BSA (m^2)	1.8±0.1	1.9±0.2	1.7±0.1	0.050
NYHA (%)				0.003*
I	18.2†	88.9	100	
II	36.4	11.1	0	
III	36.4	0	0	
IV	9.1	0	0	
Hypertension history (%)	27.3	33.3	27.3	0.945
BNP (pg/mL)	618.5 (349.5, 936.5)†	91.0 (56.0, 141.0)	144.5 (74.5, 242.5)	<0.001*
cTNI (ng/mL)	0.07 (0.05, 0.13)†	0.02 (0.01, 0.03)	0.03 (0.00, 0.05)	0.020*
eGFR (mL/min/1.73 m^2)	79±19	87±12	87±17	0.429
Limb lead low voltage in ECG (%)	27.3†	44.4§	0	0.055

Data are presented as mean ± standard deviation or median (interquartile range) if not otherwise specified. BSA (m^2) =0.0057 × height (cm) + 0.0121 × body weight (kg) + 0.0882 (male) or BSA (m^2) =0.0073 × height (cm) + 0.0127 × body weight (kg) – 0.2106 (female). eGFR was calculated by CKD-EPI equation. Limb lead low voltage: the absolute value of the limb lead voltage ≤0.5 mV. Left ventricular high voltage: V1 lead S wave and V5 or V6 lead R wave amplitude sum ≥4.0 mV (male) or 3.5 mV (female). †, P<0.05: CA-LVH *vs.* CA-NLVH group; §, P<0.05: CA-NLVH *vs.* SA group; *, P<0.05. CA-LVH, cardiac amyloidosis patients with left ventricular hypertrophy; CA-NLVH, cardiac amyloidosis patients without left ventricular hypertrophy; SA, systemic amyloidosis; BSA, body surface area; NYHA, New York Heart Association; BNP, brain natriuretic peptide; cTNI, cardiac troponin; eGFR, estimated glomerular filtration rate; ECG, electrocardiogram; CKD-EPI, Chronic Kidney Disease Epidemiology Collaboration.

Table 2 Echocardiography parameters of the three groups

Parameters	CA-LVH (n=11)	CA-NLVH (n=9)	SA (n=11)	P value
LVEDD (cm)	3.9±0.3	4.2±0.4	4.1±0.5	0.208
LVESD (cm)	2.7±0.1	2.6±0.1	2.5±0.1	0.642
LA-APD (cm)	3.9±0.8†	3.2±0.4	3.0±0.3	0.001*
IVST (cm)	1.5±0.3†	1.0±0.1	1.0±0.2	<0.001*
LVPWT (cm)	1.5 (1.4, 1.7)†	1.0 (1.0, 1.1)	0.9 (0.9, 1.1)	<0.001*
LVMI (g/m^2)	131.6±50.1†	76.9±14.6	77.3±24.2	0.001*
LVEF (%)	57.4±11.3†	69.6±3.9	68.9±4.0	0.001*
E/A	1.2 (0.9, 1.7)	0.8 (0.8, 1.0)	0.9 (0.8, 1.2)	0.221
E/E'	18.9 (15.0, 27.2)†	12.7 (11.4, 14.8)	12.3 (10.4, 14.2)	0.001*

Data are presented as mean ± standard deviation or median (interquartile range). LVMI (g/m^2) = {0.8 × 1.04 × [(IVST + LVPWT + LVEDD)^3 – LVEDD^3] + 0.6}/BSA (m^2). †, P<0.05: CA-LVH *vs.* CA-NLVH group; *, P<0.05. CA-LVH, cardiac amyloidosis patients with left ventricular hypertrophy; CA-NLVH, cardiac amyloidosis patients without left ventricular hypertrophy; SA, systemic amyloidosis; LVEDD, left ventricular end diastolic diameter; LVESD, left ventricular end systolic diameter; LA-APD, left atrium anterior-posterior diameter; IVST, interventricular septum thickness; LVPWT, left ventricular posterior wall thickness; LVMI, left ventricular mass index; LVEF, left ventricular ejection fraction; E/A, early transmitral inflow velocity to late transmitral inflow velocity ratio; E/E', mitral inflow to mitral relaxation velocity ratio.

Table 3 CMR routine parameters of the three groups

Parameter	CA-LVH (n=11)	CA-NLVH (n=9)	SA (n=11)	P value
LVEDD (cm)	4.39±0.23	4.36±0.59	4.34±0.28	0.564
Left atrium area index (cm^2/m^2)	12.5±4.8	9.5±1.8	10.5±3.5	0.195
IVST (cm)	1.37±0.17†	1.24±0.21	0.92±0.16	<0.001*
LVPWT (mm)	10.36±2.68†	8.56±3.57§	6.00±0.95	<0.001*
EDV (mL)	113.5±27.3	90.2±26.2	96.3±21.3	0.109
ESV (mL)	50.3 (34.3, 66.5)†	27.8 (25.0, 35.7)	34.9 (29.2, 37.2)	0.026*
LVEF (%)	61.2±15.2	69.2±11.6	62.9±8.0	0.312
Stroke volume (mL)	61.4±18.3	60.8±18.8	61.4±15.9	0.997
CO (mL/min)	4.6±1.2	5.1±1.2	4.6±0.7	0.066
Relative LGE volume (%)	7.4 (2.2, 11.7)	4.5 (2.8, 6.7)	–	0.210

Data are presented as mean ± standard deviation or median (interquartile range). Left atrium area index (cm^2/m^2) = left atrium area (cm^2)/BSA (m^2). Relative LGE volume = LGE volume/left ventricular volume. †, P<0.05: CA-LVH *vs.* CA-NLVH group; §, P<0.05: CA-NLVH *vs.* SA group; *, P<0.05. CMR, cardiac magnetic resonance; CA-LVH, cardiac amyloidosis patients with left ventricular hypertrophy; CA-NLVH, cardiac amyloidosis patients without left ventricular hypertrophy; SA, systemic amyloidosis; LVEDD, left ventricular end diastolic diameter; IVST, interventricular septum thickness; LVPWT, left ventricular posterior wall thickness; EDV, end of diastolic volume; ESV, end-systolic volume; LVEF, left ventricular ejection fraction; CO, cardiac output; LGE, late gadolinium enhancement; BSA, body surface area.

CMR-FT strain parameters

The CMR-FT strain parameters were shown in *Table 4*. The GRS, Basal-RS, Mid-RS, Basal-CS, Apical-LS, and endocardial and epicardial strain of CA-LVH patients were significantly impaired, compared with CA-NLVH (P<0.05). No difference in CMR-FT strain parameters was found between CA-NLVH group and SA group. All the intraclass correlation coefficient was over 0.75.

LASSO regression and ROC analysis

To early diagnosis of heart involvement (CA) with normal wall thickness, we used the data of patients in CA-NLVH and SA groups to perform LASSO regression. In this study, the following independent strain variables were included in LASSO regression: GRS, Basal-RS, Mid-RS, Apical-RS, Endo-RS, Epi-RS, GCS, Basal-CS, Mid-CS, Apical-CS, Endo-CS, Epi-CS, GLS, Basal-LS, Mid-LS, Apical-LS, Endo-LS, Epi-LS (*Figures 3*,*4*). The formula was established after screening: strain score = 0.00893 × Mid-CS + 0.02285 × Apical-RS + 0.1541 × Apical-CS + 0.33097 × Epi-CS + 0.42232 × Endo-LS. We used ROC analysis to evaluate the discriminatory efficiency of the strain score and other single strain parameter, showing the strain score yielded the greatest AUC of 0.909 (*Table 5*, *Figure 5*).

Prognosis information

One patient was lost to follow-up. The mean follow-up time of the other 30 patients was 25 months (1–45 months). Only five patients suffered outcome events during the follow-up period. All the patients with outcome events were CA patients, four were in CA-LVH group and the other one in CA-NLVH group. Seventy-one percent patients received chemotherapy and 45% patients successfully completed hematopoietic stem cell transplantation. In univariate Cox proportional hazards model, New York Heart Association (NYHA) grade, myocardial injury biomarkers, renal function and LGE volume were significantly related with the event. Routine imaging parameters, including E/E' (mitral inflow to mitral relaxation velocity ratio) [hazard ratio (HR) =1.09, P=0.040], end-systolic left ventricular volume (HR =1.04, P=0.039), left ventricular ejection fraction (LVEF) (HR =0.94, P=0.027) were also related with the event. Although without statistical difference, the strain damage had a tendency to predict poor prognosis with mid-ventricular circumferential strain with HR 1.25 (P=0.050) and strain score with HR of 1.30 (P=0.067). Due to the limited number of events in the enrolled patients, we were unable to further establish a multivariate regression model. The parameters in Cox regression were shown in *Table 6*.

Table 4 CMR-FT strain parameters of the three groups

Parameters	CA-LVH (n=11)	CA-NLVH (n=9)	SA (n=11)	P value
GRS (%)	15.6±6.9†	28.0±10.2	29.5±7.0	0.001*
Basal-RS (%)	14.4±8.5†	26.8±7.6	30.2±11.0	0.001*
Mid-RS (%)	15.0±5.7†	26.3±7.3	27.8±7.3	<0.001*
Apical-RS (%)	21.8±10.8†	36.1±16.5	34.6±10.1	0.026*
RRSR-RS	0.8±0.3	0.7±0.2	0.6±0.2	0.251
Endo-RS (%)	26.8±11.6†	36.5±7.8	40.5±7.7	0.006*
Epi-RS (%)	15.1±6.6†	20.9±3.7	24.3±4.1	0.001*
Endo-Epi (RS) (%)	11.7±5.4	15.6±5.0	16.2±4.4	0.094
Endo/Epi (RS)	1.8±0.2	1.7±0.2	1.7±0.2	0.283
GCS (%)	−13.8±4.2	−17.3±2.2	−19.3±2.6	0.001*
Basal-CS (%)	−11.8±3.9†	−15.6±2.4	−16.4±2.4	0.003*
Mid-CS (%)	−13.9±4.0	−17.4±2.5	−19.0±2.5	0.002*
Apical-CS (%)	16.4±5.2	19.8±2.9	22.6±4.3	0.008*
RRSR-CS	0.6±0.1	0.6±0.1	0.6±0.1	0.547
Endo-CS (%)	−14.7±4.8†	−16.5±4.2	−20.0±2.2	0.004*
Epi-CS (%)	−10.4±3.5†	−13.4±1.7	−15.1±1.8	0.001*
Endo-Epi (CS) (%)	−4.4±1.5	−4.6±1.4	−4.9±0.9	0.461
Endo/Epi (CS)	1.4±0.1	1.4±0.1	1.3±0.1	0.030*
GLS (%)	−6.3±2.9	−8.8±1.8	−10.4±2.8	0.003*
Basal-LS (%)	−5.1±2.2	−6.4±2.3	−7.9±3.2	0.062
Mid-LS (%)	−5.5±3.1	−8.0±2.2	−9.8±3.2	0.007*
Apical-LS (%)	−8.4±3.2†	−12.6±2.6	−13.6±2.5	<0.001*
RRSR-LS	0.8 (0.7, 1.0)	0.8 (0.8, 0.9)	0.8 (0.7, 0.9)	0.614
Endo-LS (%)	−9.3 (−10.6, 5.4)†	−11.6 (−11.9, −10.8)	−13.1 (−14.0, −11.5)	0.005*
Epi-LS (%)	−9.4 (−10.2, −5.6)†	−11.7 (−12.8, −11.4)	−12.7 (−13.4, −11.8)	0.002*
Endo-Epi (LS) (%)	−0.1±0.6	0.3±0.6	−0.2±0.5	0.103
Endo/Epi (LS)	1.0±0.1	1.0±0.1	1.0±0.1	0.435

Data are presented as mean ± standard deviation or median (interquartile range). RRSR = 3D apical peak strain/(3D basal peak strain + 3D middle peak strain); Endo-Epi = endocardial average peak strain − epicardial average peak strain (in short axis); Endo/Epi = endocardial average peak strain/epicardial average peak strain (in short axis). †, P<0.05: CA-LVH *vs.* CA-NLVH group; *, P<0.05. CMR, cardiac magnetic resonance; FT, feature tracking; CA-LVH, cardiac amyloidosis patients with left ventricular hypertrophy; CA-NLVH, cardiac amyloidosis patients without left ventricular hypertrophy; SA, systemic amyloidosis; GRS, global radial peak strain; RS, radial peak strain; Mid, mid-septal; RRSR, relative regional strain ratio; Endo, endocardial; Epi, epicardial; GCS, global circumferential peak strain; CS, circumferential peak strain; GLS, global longitudinal peak strain; LS, longitudinal peak strain; 3D, three-dimensional.

Discussion

From the analysis of this cohort of patients undergoing CMR, the major findings were as follows: (I) echocardiography has limited ability to discriminate CA-NLVH patients from SA patients; (II) the CA-LVH patients had significantly worse NYHA grade, higher BNP and myocardial injury marker, lower LVEF and worse diastolic function than CA-NLVH patients; (III) apical strain is not relatively retained in CA patients; (IV) the integrated MRI strain score can assist in the early diagnosis of CA; (V) the strain damage has a tendency to predict poor prognosis in CA patients.

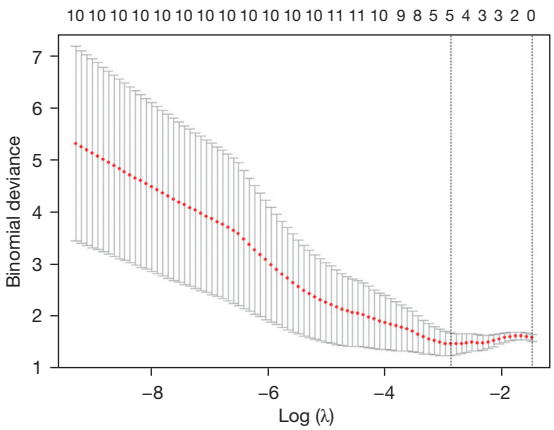

Figure 3 Selection of the tuning parameter (λ) in the LASSO model. Misclassification error for different numbers of variables revealed by the LASSO regression model. The red dots represent the value of misclassification error; the grey lines represent the SE; the two vertical dotted lines on the left and right, represent optimal values by the minimum criteria and 1-SE criteria, respectively. "λ" is the tuning parameter. The optimal λ value of 0.056 with log (λ) of –2.891 was chosen. LASSO, least absolute shrinkage and selection operator; SE, standard error.

Echocardiography in CA patients

Amyloidosis is a rare disease with an insidious onset and diverse clinical manifestations, in part due to diagnostic

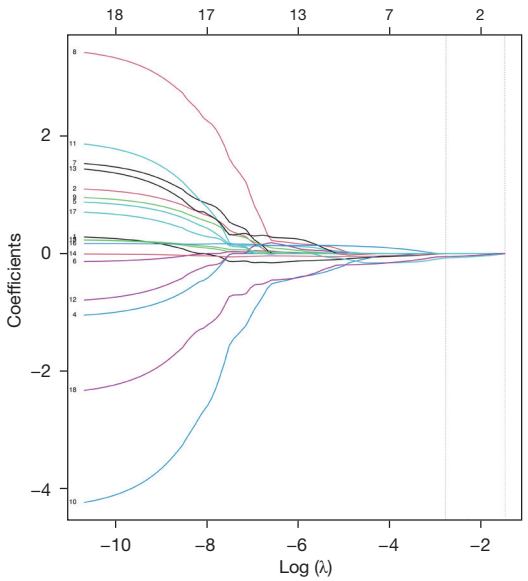

Figure 4 LASSO regression of 18 strain parameters. A vertical line was plotted at the optimal λ value, which resulted in three features with nonzero coefficients. The two vertical dotted lines on the left and right represent optimal values by the minimum criteria and 1-SE criteria, respectively. "λ" is the tuning parameter. The optimal λ value of 0.056 with log (λ) of –2.891 was chosen. 1–18 correspond to: Basal-RS, Mid-RS, Apical-RS, GRS, Endo-RS, Epi-RS, Basal-CS, Mid-CS, Apical-CS, GCS, Endo-CS, Epi-CS, Basal-LS, Mid-LS, Apical-LS, GLS, Endo-LS, Epi-LS. LASSO, least absolute shrinkage and selection operator; SE, standard error; RS, radial peak strain; Mid, mid-septal; GRS, global radial peak strain; Endo, endocardial; Epi, epicardial; CS, circumferential peak strain; GCS, global circumferential peak strain; LS, longitudinal peak strain; GLS, global longitudinal peak strain.

Table 5 ROC analysis of strain score and other single strain parameters

Parameter	AUC	95% CI	Best threshold	Specificity	Sensitivity	Accuracy	P value*
Strain score	0.909	0.775–1.000	–12.387	0.818	1.000	0.900	–
Epi-CS	0.778	0.560–0.995	–14.286	0.727	0.778	0.750	0.209
Endo-Epi (LS)	0.778	0.565–0.991	–0.121	0.727	0.778	0.750	0.282
Endo/Epi (LS)	0.768	0.547–0.988	1.009	0.727	0.778	0.750	0.265

*, compared with strain score. Endo-Epi = endocardial average peak strain – epicardial average peak strain (in short axis); Endo/Epi = endocardial average peak strain/epicardial average peak strain (in short axis). ROC, receiver operating characteristic; AUC, area under the curve; CI, confidence interval; Endo, endocardial; Epi, epicardial; CS, circumferential peak strain; LS, longitudinal peak strain.

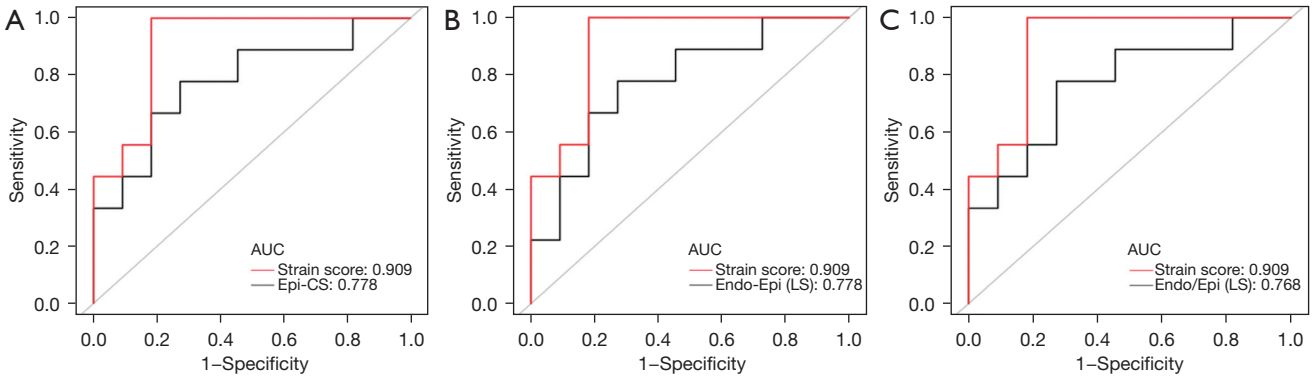

Figure 5 ROC curve analysis for strain score and other single strain parameters. (A) Strain score compared with Epi-CS; (B) strain score compared with Endo-Epi (LS); (C) strain score compared with Endo/Epi (LS). Endo-Epi = endocardial average peak strain – epicardial average peak strain (in short axis); Endo/Epi = endocardial average peak strain/epicardial average peak strain (in short axis). AUC, area under the curve; Endo, endocardial; Epi, epicardial; CS, circumferential peak strain; LS, longitudinal peak strain; ROC, receiver operating characteristic.

omissions and delays. If patients are diagnosed early and treated promptly, the prognosis can be significantly improved. All this means that there is an unmet medical need for early detection and diagnosis of amyloidosis and cardiac involvement.

In addition to traditional ECG and myocardial injury markers, cardiovascular imaging (echocardiography, CMR) plays a vital role in the early diagnosis of CA (21). Compared with other methods, the advantages of echocardiography include convenience, affordability, and high accessibility. The drawbacks include the low tissue resolution, uncontrollable image quality, and relatively fixed but not comprehensive observation angle of the myocardium (22). In the population enrolled in this study, it is easy to find those who did not have myocardial hypertrophy on echocardiography but who did have heart involvement. Therefore, echocardiography has limited diagnostic value for CA patients with normal left ventricular wall thickness.

Clinical characteristics of CA patients

Our study found that the CA-LVH group had worse NYHA grade, higher BNP and myocardial injury marker, lower LVEF and worse diastolic function compared with the CA-NLVH group. The main reasons are as follows: firstly, the heart of CA-LVH has a higher amyloid burden than CA-NLVH and amyloid deposition impairs myocardial microcirculatory function, decreased left ventricular systolic function and release of myocardial injury markers (23). Finally, in patients with progressive disease, diastolic dysfunction leads to atrial dilatation and the release of large amounts of natriuretic peptides. However, the above indicators are not sufficient to discriminate the CA-NLVH group from the SA group, so the above indicators do not have the value of early detection of cardiac involvement.

By comparing the results of conventional magnetic resonance parameters, it was found that the end-systolic left ventricular volume was larger in the CA-LVH group compared with the CA-NLVH group, whereas the end-systolic diameter was not significantly different, suggesting that in addition to the diameter, the volume was of significant clinical relevance as well. Left ventricular posterior wall thickness was the only indicator of conventional magnetic resonance parameters to discriminate between the CA-NLVH and SA groups, suggesting that the higher tissue resolution of CMR compared with echocardiography may avoid underestimation of left ventricular posterior wall thickness (24). The European Society of Cardiology recently stated that clinical suspicion of CA is required for ventricular septal hypertrophy (equal to or thicker than 12 mm) (25).

Assessment of CA by CMR-FT

In our study, the apical longitudinal strain appears to decrease, while the strain at the base and the middle section remains. This seems to be a new finding, which is different from the results of previous studies (26). However, there are few studies on the cardiac strain pattern based

Table 6 Prognosis Cox regression of different parameters

Parameters	Event group (n=5)	Without event group (n=25)	HR (95% CI)	P value
NYHA grade ≥III (%)	60	4	14.29 (2.34–87.34)	<0.01*
Log (BNP)	2.9±0.4	2.1±0.5	20.05 (2.21–182.36)	0.008*
Log (cTNI)	−1.0±0.3	−1.7±0.7	11.59 (1.03–130.36)	0.047*
eGFR (mL/min/1.73 m^2)	65.9±18.4	87.8±13.5	0.92 (0.86–0.98)	0.011*
E/E'	23.4±9.5	14.2±5.9	1.09 (1.00–1.18)	0.040*
ESV in CMR (mL)	56.4±23.0	36.1±15.6	1.04 (1.00–1.08)	0.039*
LVEF in CMR (%)	51.6±16.1	63.8±7.9	0.94 (0.88–0.99)	0.027*
Relative LGE volume (%)	12.3±12.5	6.0±3.3	1.11 (1.02–1.20)	0.012*
GRS (%)	16.7±8.4	26.1±9.7	0.91 (0.81–1.01)	0.086
Basal-RS (%)	14.9±11.5	25.7±10.7	0.91 (0.83–1.01)	0.075
Mid-RS (%)	15.5±7.4	24.5±8.5	0.88 (0.77–1.01)	0.060
Apical-RS (%)	22.4±11.9	32.1±14.0	0.95 (0.88–1.03)	0.206
RRSR-RS	0.79±0.24	0.66±0.23	5.56 (0.16–199.20)	0.347
Endo-RS (%)	27.6±14.5	36.5±9.4	0.94 (0.87–1.02)	0.125
Epi-RS (%)	16.2±8.9	21.2±5.4	0.90 (0.78–1.03)	0.132
Endo-Epi (RS) (%)	11.5±5.8	15.3±4.9	0.88 (0.74–1.06)	0.175
Endo/Epi (RS)	1.72±0.10	1.73±0.19	0.54 (0.00–79.26)	0.807
GCS (%)	−13.4±5.4	−17.5±3.3	1.23 (0.99–1.53)	0.057
Basal-CS (%)	−11.5±4.6	−15.2±3.1	1.24 (0.99–1.16)	0.059
Mid-CS (%)	−13.5±5.3	−17.4±3.2	1.25 (1.0–1.57)	0.050
Apical-CS (%)	−16.1±6.8	−20.4±4.4	1.16 (0.96–1.39)	0.121
RRSR-CS	0.64±0.10	0.63±0.10	2.98 (0.00–20,381.25)	0.809
Endo-CS (%)	−15.0±5.7	−18.5±3.2	1.20 (0.97–1.48)	0.090
Epi-CS (%)	−10.8±4.6	−13.5±2.6	1.24 (0.96–1.61)	0.100
Endo-Epi (CS) (%)	−4.2±1.1	−5.0±1.1	1.71 (0.73–3.98)	0.211
Endo/Epi (CS)	1.41±0.08	1.38±0.10	17.75 (0.00–107,290.81)	0.519
GLS (%)	−6.7±3.5	−8.9±2.9	1.25 (0.92–1.69)	0.157
Basal-LS (%)	−5.0±2.1	−6.8±2.9	1.23 (0.87–1.73)	0.248
Mid-LS (%)	−6.4±3.7	−8.2±3.2	1.18 (0.87–1.59)	0.285
Apical-LS (%)	−8.7±4.2	−12.2±3.2	1.26 (0.98–1.63)	0.069
RRSR-LS	0.77±0.08	0.89±0.30	0.09 (0.00–34.73)	0.425
Endo-LS (%)	−8.4±4.6	−11.5±2.7	1.25 (0.99–1.57)	0.062
Epi-LS (%)	−8.5±4.4	−11.5±2.5	1.27 (0.99–1.62)	0.063
Endo-Epi (LS) (%)	0.0±0.5	−0.1±0.6	1.32 (0.33–5.25)	0.692
Endo/Epi (LS)	0.99±0.07	1.00±0.08	0.28 (0.00–9,536.99)	0.811
Strain score	–	–	1.30 (0.98–1.73)	0.067

Data are presented as mean ± standard if not otherwise specified. *, P<0.05. Endo-Epi = endocardial average peak strain − epicardial average peak strain (in short axis); Endo/Epi = endocardial average peak strain/epicardial average peak strain (in short axis). HR, hazard ratio; CI, confidence interval; NYHA, New York Heart Association; BNP, brain natriuretic peptide; cTNI, cardiac troponin; eGFR, estimated glomerular filtration rate; E/E', mitral inflow to mitral relaxation velocity ratio; ESV, end-systolic volume; CMR, cardiac magnetic resonance; LVEF, left ventricular ejection fraction; LGE, late gadolinium enhancement; GRS, global radial peak strain; RS, radial peak strain; Mid, mid-septal; RRSR, relative regional strain ratio; Endo, endocardial; Epi, epicardial; GCS, global circumferential peak strain; CS, circumferential peak strain; GLS, global longitudinal peak strain; LS, longitudinal peak strain.

on CMR imaging in patients with CA, and the results are controversial. The results of the myocardial strain study show that the radial strain and the circumferential strain have the classic apical retention characteristics, that is, with the gradual deposition of amyloid, the radial and circumferential strain of the basal and middle segments show a significant drop, but the apical strain is still relatively retained (27). Both the epicardial and endocardial strain have shown a synchronous reduction, which is also consistent with the characteristic that amyloidosis is often a full-thickness infiltration (28). Nevertheless, Williams *et al.* found that there was no statistical difference in apical to basal LS ratios between patients with CA and patients with hypertrophic cardiomyopathy, and the sensitivity of using RRSR to diagnose CA was low (26). Pandey *et al.* noted that global, basal, mid-ventricular and apical strain values were impaired in patients with CA compared to healthy controls, but did not find apical retention characteristics in patients with CA (29). Possible reasons include some patients with CA may not have apical sparing, apical retention characteristics will gradually decrease with the gradient of disease progression, the apical longitudinal strain should be easily damaged, and the bias might be caused by the small sample size. Therefore, a study with a larger sample size or longitudinal follow-up or both of myocardial amyloidosis may be able to reveal these patterns. Therefore, clinicians should be cautious when using apical retention characteristics to exclude CA patients. Due to the limited number of patients enrolled, we were unable to find the significant difference in CMR-FT strain parameters between CA-NLVH and SA.

Our study is the first to use LASSO regression analysis, which screened diagnostic information for 18 strain parameters derived from CMR images and generated a final score by integrating five strain parameters. When evaluating the discriminatory efficiency in patients without ventricular wall thickness using ROC analysis, the strain score yielded the greatest AUC of 0.909. LASSO regression is suitable for the regression of high-dimensional data. This result suggests that strain score may improve the efficiency of early diagnosis and differential diagnosis in patients with SA. CA may weaken myocardial strain of different types in different regions, so the diagnostic efficiency of a single strain index may be limited. Although the AUC of strain score in our study is 0.909, which is higher than any single strain index, but we must be careful when interpreting the result because of the small sample size. We need to verify and adjust this strain score in future studies with larger sample size.

Prognostic factors of SA

Possible prognostic factors in patients with SA were explored in this study. The incidence of outcome events in our study is lower than that reported in the literature (30). Only five patients experienced outcome events during the follow-up period. Seventy-one percent of patients received chemotherapy and 45% of patients successfully completed hematopoietic stem cell transplantation, which may explain the better prognosis in our study. All outcome events were reported by CA patients. Four patients were in the CA-LVH group and one in the CA-NLVH group. This result suggests that even without wall thickening, mild cardiac involvement still affects prognosis. Thus, there is a great unmet medical need for early diagnosis of amyloid cardiac involvement. Our study found that advanced NYHA grade, high BNP and myocardial injury markers, low eGFR, and high E/E' are all potential risk factors for poor prognosis and these factors also play an important role in staging the disease, guiding treatment and prognostic assessment (31,32), which is also consistent with current clinical knowledge. With regard to CMR, the important value of LGE in assessing the prognosis of CA patients has been reaffirmed. In addition, the left ventricular end-systolic volume is also an important indicator, which we need to pay more attention to in further research. In addition to early diagnosis, strain also has its value in predicting prognosis (30,33). Previous studies have shown that LS is significantly associated with CA prognosis compared to biomarkers (34-36). Although without statistical difference, strain damage had a tendency to predict poor prognosis: mid-ventricular circumferential strain with HR of 1.25 (P=0.050) and strain score with HR of 1.30 (P=0.067). Limited by the small sample size and low event rate, we did not conduct multivariate regression analysis in this study, which will be performed in future studies with large sample sizes.

Limitation

This study still has many limitations. First of all, given the low incidence of amyloidosis, the sample size of this study is small, which may lead to insufficient power of the results, such as the 95% CI of NYHA grade ≥III, BNP and cTNI were too large. Further expansion of the study is necessary to confirm the results of this research. Secondly, the majority of patients enrolled in this study were diagnosed

with AL amyloidosis. Only one case of AA amyloidosis was included in the CA-NLVH group. Further studies should include TTR amyloidosis patients to make the population more representative. In addition, the use of LGE alone to diagnose cardiac involvement in amyloidosis in this study affected the accuracy of the diagnosis. Further studies should combine other techniques of CMR such as ECV, T1 mapping, to aid in the assessment of cardiac involvement in patients with amyloidosis. Finally, in the prognostic analysis of this study, although the high-risk CA population was followed up for 2 years, multivariate regression analysis was not performed due to the high treatment rate of the selected population and therefore low incidence of events. The sample size still needs to be further expanded to resolve this dilemma.

Conclusions

In this study, the analysis of CMR strain by FT found that patients with myocardial amyloidosis with mean left ventricular thickness ≤12 mm had no significant difference in overall, basal, mid, apical, and endocardial strain compared with patients with amyloidosis without myocardial involvement. With ventricular thickening and disease progression, the overall, endocardial, and epicardial strains significantly decreased in patients with myocardial amyloidosis. The integrated MRI strain score is a useful tool to identify early myocardial involvement in amyloidosis. Besides some clinical characteristics and some traditional imaging indices, strain damage had a tendency to predict poor prognosis. This dilemma needs to be resolved in further large clinical trials.

Acknowledgments

The authors thank all the staff in the Department of Cardiology and Department of Radiology, Peking University First Hospital for their valuable contributions to this study.
Funding: None.

Footnote

Reporting Checklist: The authors have completed the STROBE reporting checklist. Available at https://cdt.amegroups.com/article/view/10.21037/cdt-23-205/rc

Data Sharing Statement: Available at https://cdt.amegroups.com/article/view/10.21037/cdt-23-205/dss

Peer Review File: Available at https://cdt.amegroups.com/article/view/10.21037/cdt-23-205/prf

Conflicts of Interest: All authors have completed the ICMJE uniform disclosure form (available at https://cdt.amegroups.com/article/view/10.21037/cdt-23-205/coif). The authors have no conflicts of interest to declare.

Ethical Statement: The authors are accountable for all aspects of the work in ensuring that questions related to the accuracy or integrity of any part of the work are appropriately investigated and resolved. The study was conducted in accordance with the Declaration of Helsinki (as revised in 2013). The study was approved by Peking University First Hospital Ethics Committee (No. 2020keyan141). Written consent was waived owing to the minimal patient risk in accordance with the relevant guidelines and regulations of Peking University First Hospital Ethics Committee, but all patients were consented for the procedure.

References

1. Wechalekar AD, Gillmore JD, Hawkins PN. Systemic amyloidosis. Lancet 2016;387:2641-54.
2. Magy-Bertrand N, Dupond JL, Mauny F, et al. Incidence of amyloidosis over 3 years: the AMYPRO study. Clin Exp Rheumatol 2008;26:1074-8.
3. Falk RH, Alexander KM, Liao R, et al. AL (Light-Chain) Cardiac Amyloidosis: A Review of Diagnosis and Therapy. J Am Coll Cardiol 2016;68:1323-41.
4. Maurer MS, Elliott P, Comenzo R, et al. Addressing Common Questions Encountered in the Diagnosis and Management of Cardiac Amyloidosis. Circulation 2017;135:1357-77.
5. Oda S, Utsunomiya D, Nakaura T, et al. Identification and

Assessment of Cardiac Amyloidosis by Myocardial Strain Analysis of Cardiac Magnetic Resonance Imaging. Circ J 2017;81:1014-21.
6. Siddiqi OK, Ruberg FL. Cardiac amyloidosis: An update on pathophysiology, diagnosis, and treatment. Trends Cardiovasc Med 2018;28:10-21.
7. Bhatti S, Watts E, Syed F, et al. Clinical and prognostic utility of cardiovascular magnetic resonance imaging in myeloma patients with suspected cardiac amyloidosis. Eur Heart J Cardiovasc Imaging 2016;17:970-7.
8. Murtagh B, Hammill SC, Gertz MA, et al. Electrocardiographic findings in primary systemic amyloidosis and biopsy-proven cardiac involvement. Am J Cardiol 2005;95:535-7.
9. Takashio S, Yamamuro M, Izumiya Y, et al. Diagnostic utility of cardiac troponin T level in patients with cardiac amyloidosis. ESC Heart Fail 2018;5:27-35.
10. Baggiano A, Boldrini M, Martinez-Naharro A, et al. Noncontrast Magnetic Resonance for the Diagnosis of Cardiac Amyloidosis. JACC Cardiovasc Imaging 2020;13:69-80.
11. Licordari R, Trimarchi G, Teresi L, et al. Cardiac Magnetic Resonance in HCM Phenocopies: From Diagnosis to Risk Stratification and Therapeutic Management. J Clin Med 2023;12:3481.
12. Fontana M, Chung R, Hawkins PN, et al. Cardiovascular magnetic resonance for amyloidosis. Heart Fail Rev 2015;20:133-44.
13. Austin BA, Tang WH, Rodriguez ER, et al. Delayed hyper-enhancement magnetic resonance imaging provides incremental diagnostic and prognostic utility in suspected cardiac amyloidosis. JACC Cardiovasc Imaging 2009;2:1369-77.
14. Messroghli DR, Moon JC, Ferreira VM, et al. Clinical recommendations for cardiovascular magnetic resonance mapping of T1, T2, T2* and extracellular volume: A consensus statement by the Society for Cardiovascular Magnetic Resonance (SCMR) endorsed by the European Association for Cardiovascular Imaging (EACVI). J Cardiovasc Magn Reson 2017;19:75.
15. Martinez-Naharro A, Abdel-Gadir A, Treibel TA, et al. CMR-Verified Regression of Cardiac AL Amyloid After Chemotherapy. JACC Cardiovasc Imaging 2018;11:152-4.
16. Modin D, Andersen DM, Biering-Sørensen T. Echo and heart failure: when do people need an echo, and when do they need natriuretic peptides? Echo Res Pract 2018;5:R65-79.
17. Marwick TH, Shah SJ, Thomas JD. Myocardial Strain in the Assessment of Patients With Heart Failure: A Review. JAMA Cardiol 2019;4:287-94.
18. Chitiboi T, Axel L. Magnetic resonance imaging of myocardial strain: A review of current approaches. J Magn Reson Imaging 2017;46:1263-80.
19. van Everdingen WM, Zweerink A, Nijveldt R, et al. Comparison of strain imaging techniques in CRT candidates: CMR tagging, CMR feature tracking and speckle tracking echocardiography. Int J Cardiovasc Imaging 2018;34:443-56.
20. Edvardsen T, Klaeboe LG. Imaging and heart failure: myocardial strain. Curr Opin Cardiol 2019;34:490-4.
21. Khanna S, Wen I, Bhat A, et al. The Role of Multi-modality Imaging in the Diagnosis of Cardiac Amyloidosis: A Focused Update. Front Cardiovasc Med 2020;7:590557.
22. Koyama J, Ikeda S, Ikeda U. Echocardiographic assessment of the cardiac amyloidoses. Circ J 2015;79:721-34.
23. Kociol RD, Pang PS, Gheorghiade M, et al. Troponin elevation in heart failure prevalence, mechanisms, and clinical implications. J Am Coll Cardiol 2010;56:1071-8.
24. Lee GY, Kim K, Choi JO, et al. Cardiac amyloidosis without increased left ventricular wall thickness. Mayo Clin Proc 2014;89:781-9.
25. Garcia-Pavia P, Rapezzi C, Adler Y, et al. Diagnosis and treatment of cardiac amyloidosis: a position statement of the ESC Working Group on Myocardial and Pericardial Diseases. Eur Heart J 2021;42:1554-68.
26. Williams LK, Forero JF, Popovic ZB, et al. Patterns of CMR measured longitudinal strain and its association with late gadolinium enhancement in patients with cardiac amyloidosis and its mimics. J Cardiovasc Magn Reson 2017;19:61.
27. Phelan D, Collier P, Thavendiranathan P, et al. Relative apical sparing of longitudinal strain using two-dimensional speckle-tracking echocardiography is both sensitive and specific for the diagnosis of cardiac amyloidosis. Heart 2012;98:1442-8.
28. Bhatti S, Vallurupalli S, Ambach S, et al. Myocardial strain pattern in patients with cardiac amyloidosis secondary to multiple myeloma: a cardiac MRI feature tracking study. Int J Cardiovasc Imaging 2018;34:27-33.
29. Pandey T, Alapati S, Wadhwa V, et al. Evaluation of Myocardial Strain in Patients With Amyloidosis Using Cardiac Magnetic Resonance Feature Tracking. Curr Probl Diagn Radiol 2017;46:288-94.
30. Illman JE, Arunachalam SP, Arani A, et al. MRI feature tracking strain is prognostic for all-cause mortality in AL amyloidosis. Amyloid 2018;25:101-8.

31. Gillmore JD, Damy T, Fontana M, et al. A new staging system for cardiac transthyretin amyloidosis. Eur Heart J 2018;39:2799-806.
32. Perfetto F, Zampieri M, Fumagalli C, et al. Circulating biomarkers in diagnosis and management of cardiac amyloidosis: a review for internist. Intern Emerg Med 2022;17:957-69.
33. Wan K, Sun J, Yang D, et al. Left Ventricular Myocardial Deformation on Cine MR Images: Relationship to Severity of Disease and Prognosis in Light-Chain Amyloidosis. Radiology 2018;288:73-80.
34. Cohen OC, Ismael A, Pawarova B, et al. Longitudinal strain is an independent predictor of survival and response to therapy in patients with systemic AL amyloidosis. Eur Heart J 2022;43:333-41.
35. Huntjens PR, Zhang KW, Soyama Y, et al. Prognostic Utility of Echocardiographic Atrial and Ventricular Strain Imaging in Patients With Cardiac Amyloidosis. JACC Cardiovasc Imaging 2021;14:1508-19.
36. Lee Chuy K, Drill E, Yang JC, et al. Incremental Value of Global Longitudinal Strain for Predicting Survival in Patients With Advanced AL Amyloidosis. JACC CardioOncol 2020;2:223-31.

Cite this article as: Hou W, Wang Z, Huang J, Fan F, Yang F, Qiu L, Zhao K, Qiu J, Yang Y, Ma W, Gong Y, Hong T. Early diagnostic and prognostic value of myocardial strain derived from cardiovascular magnetic resonance in patients with cardiac amyloidosis. Cardiovasc Diagn Ther 2023;13(6):979-993. doi: 10.21037/cdt-23-205

